Impedance measurement to assess epicardial fat prior to RF intraoperative cardiac ablation: feasibility study using a computer model

Ana González-Suárez[1], Fernando Hornero[2] and Enrique J Berjano[1]

[1] Biomedical Synergy, Electronic Engineering Department, Universidad Politécnica de Valencia, Camino de VeraValencia, Spain
[2] Department of Cardiac Surgery, Consortium University General Hospital, Valencia, Spain

E-mail: angonsua@posgrado.upv.es

Abstract
Radiofrequency (RF) cardiac ablation is used to treat certain types of arrhythmias. In the epicardial approach, efficacy of RF ablation is uncertain due to the presence of epicardial adipose tissue interposed between the ablation electrode and the atrial wall. We planned a feasibility study based on a theoretical model in order to assess a new technique to estimate the quantity of fat by conducting bioimpedance measurements using a multi-electrode probe. The Finite Element Method was used to solve the electrical problem. The results showed that the measured impedance profile coincided approximately with the epicardial fat profile measured under the probe electrodes and also that the thicker the epicardial fat, the higher the impedance values. When lateral fat width was less than 4.5 mm, the impedance values altered, suggesting that measurements should always be conducted over a sizeable fat layer. We concluded that impedance measurement could be a practical method of assessing epicardial fat prior to RF intraoperative cardiac ablation, i.e. "to map" the amount of adipose tissue under the probe.

Keywords: Atrial fibrillation, bioimpedance measurement, cardiac ablation, computational modeling, epicardial ablation, epicardial fat, finite element method, theoretical model.

1. Introduction

Radiofrequency (RF) cardiac ablation can be used to treat certain types of arrhythmias, such as atrial fibrillation (AF), which is a common arrhythmia and an important public health problem due to its clinical prevalence and morbid-mortality (Kannel *et al* 1998, Benjamin *et al* 1994, Wolf *et al* 1991). The use of both surgical (intraoperative) and percutaneous (via a catheter) RF ablation to treat AF is increasing, in spite of the lack of accurate knowledge of the mechanisms involved. The effectiveness of surgical ablation is 70-80%, regardless of the kind of energy used (Khargi *et al* 2005, Cox *et al* 1996, Nakajima *et al* 2002). It is has been hypothesized that the early post-ablation recurrence of AF probably depends on the incomplete transmurality of the lesion (Miyagi *et al* 2009). In fact, histological analyses of lesions have shown that 25-30%

are non transmural cases (Santiago *et al* 2003a, b, Deneke *et al* 2005). In the epicardial approach, i.e. when the energy to create the thermal lesion is applied on the epicardial surface, the efficacy of RF ablation is uncertain, due to the varying presence of epicardial adipose tissue interposed between the ablation electrode and target site, i.e. the atrial wall (Miyagi *et al* 2009, Berjano and Hornero 2004). This is probably due to the electrical conductivity of the fat being lower than that of atrial tissue (0.02 and 0.4-0.6 S/m respectively) (González-Suárez *et al* 2010). In addition, since fat has a lower thermal conductivity (0.2 W/m·K) than atrial tissue (0.7 W/m·K), the presence of this fat layer also probably has a negative impact on creating a transmural lesion, regardless of the type of energy used. In order to maximize effectiveness of epicardial RF ablation therapy, Dumas et al (2008) used impedance measurements to predict completeness of lesions. Moreover, different types of energy are currently being researched, such as high intensity focused ultrasound (HIFU) (Mitnovetsky *et al* 2009), microwave (Pruitt *et al* 2007), laser (Hong *et al* 2007) and cryoablation (Ba *et al* 2008) in order to achieve optimum epicardial lesions in atrial tissue. We have previously used computer models to study the capability of different procedural techniques (different electrode designs and protocols for delivering RF power) to ablate atrial tissue in the presence of epicardial fat (González-Suárez *et al* 2010). Since our results showed the difficulty of ablating the atrial wall in the presence of thick fat layers (4-5 mm), it would be desirable to have a technique available to estimate the quantity of overlying epicardial fat prior to ablation. We therefore propose a new technique based on impedance measurements to assess epicardial fat thickness. Figure 1 shows the physical situation of the proposed technique, which is based on a multi-electrode probe placed over the epicardial surface. Our hypothesis is as follows: the electrical impedance measured between two or more electrodes of the probe could be closely related to the quantity of fat under the electrodes. For example, the impedance measured on a thin fat layer (Z_2) would be lower than on a thick layer (Z_1). An impedance profile (i.e. a set of impedance values, Z_1, Z_2...) could therefore be used to obtain a fat profile.

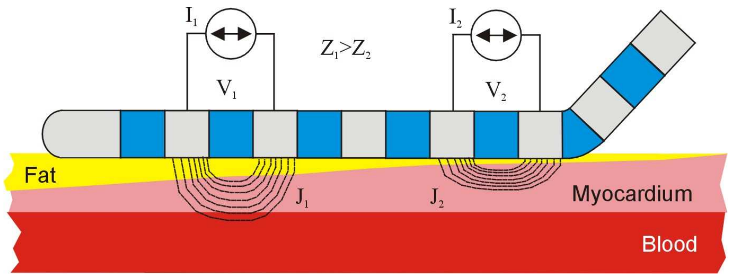

Figure 1. Physical situation considered in the study of the estimation of the epicardial fat profile. The idea is based on the fact that the electrical impedance measured between two or more electrodes of the probe could be strongly related to the quantity of fat under the electrodes. For example, the impedance measured on a thin fat layer ($Z_2 = V_2/I_2$) would be lower than on a thick fat layer ($Z_1 = V_1/I_1$).

Theoretical modeling has previously been used to assess the feasibility of new medical techniques and devices (Berjano and Hornero 2006, 2005). In other words, this methodological approach has been employed as a concept proof. In our case, we designed a computer modeling study to determine the feasibility of the proposed technique. In this type of study it is also very important to assess the effect of external parameters, i.e. those affecting the final outcome when the device or technique is employed in a real stage. This can be done both to minimize their effects (because they involve an undesirable dispersion in the performance of the device) and to find optimum values for improving the performance of the device or technique. As computer modeling can also be used for this task, we used it to determine how anatomical factors (e.g. presence or lack of fat near the measuring electrodes) could affect the accuracy of the estimation of fat thickness.

2. Methods

2.1. Description of the theoretical model

Figure 2 shows the proposed theoretical model, which represents a straight probe over three parallel sections of tissue: epicardial fat, atrial wall and circulating blood, with thicknesses F, A and B, respectively. The probe was considered to have a rectangular section and 3 mm thickness, 1 mm in height and L total length. It consisted of 8 (stainless steel) electrodes 3 mm in length with 4 mm plastic segments (polyurethane) between them. The first and last sections of the probe were also constructed of polyurethane with a length P (see Figure 2). Since there is a symmetry plane, only half of the model was considered.

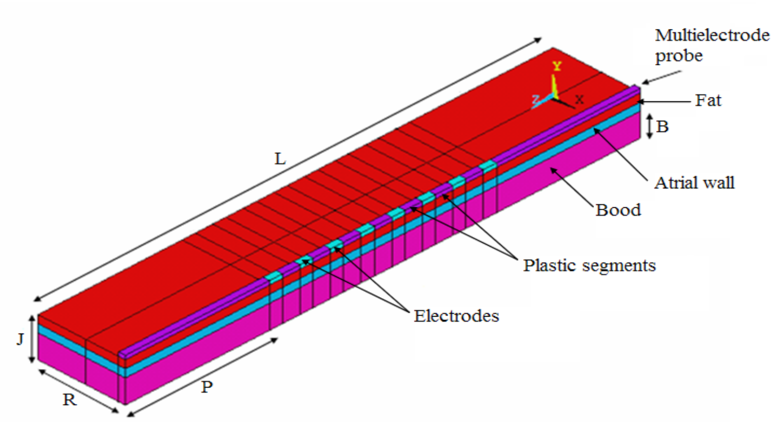

Figure 2. Theoretical model proposed with a uniform fat profile. Since there is a symmetrical plane, the model only includes half of all probe-tissues. R (half of the model), B (blood thickness) and L (length of the multielectrode probe): outer dimensions of the model; J: model thickness composed of three layers (F: epicardical fat thickness; A: atrial wall thickness; B: blood volume); P: distance from the first and last electrodes to the boundaries of the model.

2.2. Impedance measuring technique

We modeled impedance measurements using a tetrapolar (quadripolar) technique, i.e. an electrical current was injected between two outer electrodes and the voltage was measured between two inner electrodes (see Figure 3). This technique reduces the effect of electrode impedance and gives better accuracy than the bipolar technique

(Grimmes and Martinsen 2008, Geddes 1989). A total of 5 impedance measurements were obtained: Z_A, Z_B, Z_C, Z_D and Z_E, where Z_A was the ratio between the voltage measured between electrodes 2 and 3 (V_{23}) and the current applied through electrodes 1 and 4 (I_{14}), i.e. $Z_A = V_{23}/I_{14}$; Z_B was the ratio between the voltage measured between electrodes 3 and 4 (V_{34}) and the current injected through electrodes 2 and 5 (I_{25}), i.e. $Z_B = V_{34}/I_{25}$; etc. In this way, the value of Z_A is related to the electrical conductivity of the tissue beneath electrodes 2 and 3, Z_B of the tissues beneath the electrodes 3 and 4, and so on until all the tissue under the probe has been “mapped”.

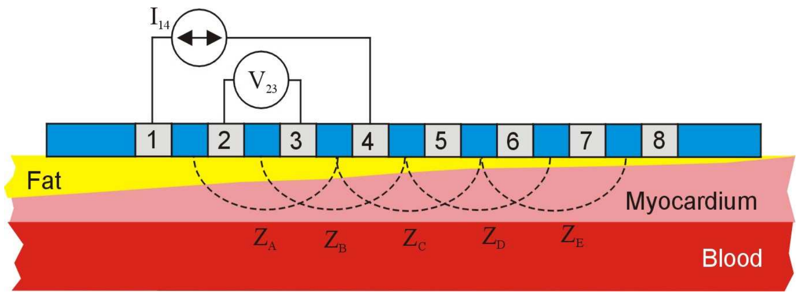

Figure 3. The impedance measurements were conducted by using a tetrapolar technique, i.e. an electrical current was injected between two outer electrodes, and an electrical voltage was measured between two inner electrodes. For instance, the figure illustrates by using electrodes 1 and 4 to inject current and electrodes 2 and 3 to pick up voltage, how it is possible "to map" the impedance Z_A (i.e. V_{23}/I_{14}) corresponding with the tissue zone lying beneath electrodes 2 and 3; Z_B (V_{34}/I_{25}) with the zone beneath electrodes 3 and 4, and consecutively until all the tissue under the probe has been “mapped”.

2.3. Governing equations

In a preliminary computer modeling study, we assessed the effect of changing the measuring frequency (between 10 and 10 MHz) on the capability of this technique to estimate the epicardial fat profile. We found that 1 MHz would be the best option, since the higher value (10 MHz) would show up practical problems (González-Suárez *et al* 2009). The value of electrical conductivity (σ) for atrial tissue therefore was a frequency of 1 MHz. The biological medium at this frequency can be considered almost totally resistive, since the displacement currents are much less important than conduction currents. The only characteristic considered for the materials employed in the model was electrical conductivity (Gabriel *et al* 1996): 0.025 S/m for the adipose tissue, 0.4 S/m for the atrial tissue, 0.99 S/m for the blood, 7.4×10^6 S/m for the electrodes (stainless steel) and 10^{-5} S/m for the plastic section of the probe (polyurethane). A quasi-static approach was employed to solve the electrical problem (Doss 1982). The Laplace Equation governed the physical phenomenon.

We used ANSYS version 10.0 (ANSYS, Canonsburg, PA, USA) to build theoretical models and solved them by means of the Finite Element Method (FEM). The SOLID69 element (linear isoparametric type) was used to solve the static electrical problem. This means that although the electrical variables in the theoretical model (voltage and current) are DC values, they correspond with the root-mean-square value of the AC signals in a real situation.

2.4. Boundary conditions

A Neumann boundary condition of null electrical current was used both on the symmetry plane and at the rest of the boundaries. To obtain each impedance measurement, we set a value of 1 A at a node inside one current injection electrode, and a value of −1 A at a node inside the other current injection electrode (Neumann boundary conditions (Brankov *et al* 2000)). Obviously, in a real situation, lower electrical current values would be used. A Dirichlet boundary condition of null electrical voltage was set at the nodes containing electrodes to pick up the electrical voltage. The voltage value of the other pick-up electrode corresponded directly with the impedance value.

2.5. Construction of the numerical model

The outer dimensions R, B and L (see Figure 2) were calculated by means of a convergence test in order to avoid boundary effects, i.e. they should be large enough to model an unlimited volume. A convergence test was also performed to obtain the correct spatial resolution (i.e. minimum meshing size). Discretization was spatially heterogeneous: the finest zone was always the electrode-tissue interface, since it is known that this contains the largest voltage gradient. The meshing size was gradually increased with distance from the interface. In these convergence tests the value of the electrical impedance (Z) was used as a control parameter. First, we considered a tentative spatial resolution of 0.3 mm at the electrode-tissue interface. To determine the appropriate values of R, B and L we conducted a computer analysis by increasing the value of these parameters by equal amounts. When the difference between the impedance and the same parameter in the previous simulation was less than 0.5%, we considered the former values to be appropriate. Finally, we conducted a convergence test to determine the appropriate spatial resolution. The optimum spatial discretization was then achieved by refining the mesh in this zone so that Z was within 0.5% of the value obtained from the previous refinement step.

2.6. Effect of different fat profiles

To assess the effect of the overlying epicardial fat on the impedance measurements, we considered four shapes of fat profile: uniform (which corresponds with the model initially shown, see Figure 2), linear, convex and concave (see Figure 4). The atrial wall and blood layer had a thickness of 2 and 6 mm, respectively, in all the models. For the uniform profile, we studied the effect of changing the epicardial fat layer thickness (F) from 1 to 6 mm. For the other three profiles, we considered a variation of maximum fat thickness from 6 to 1 mm, with minimum fat thickness at 0.1 mm.

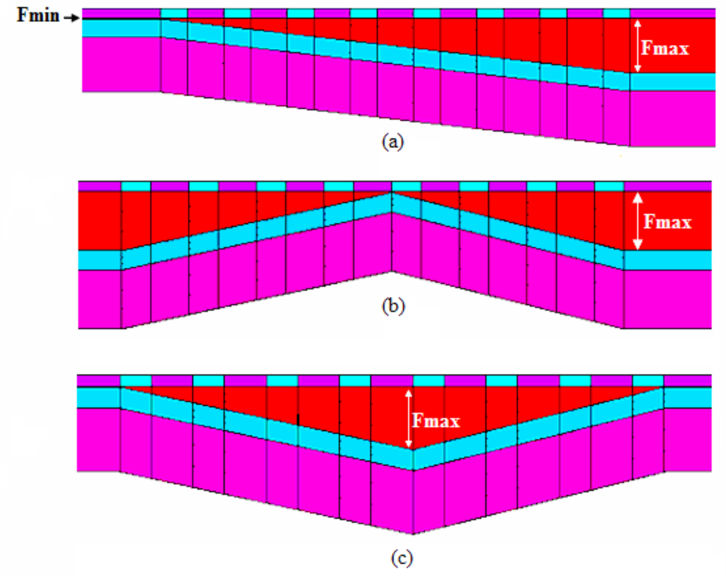

Figure 4. Theoretical models with different epicardial fat profiles: (a) linear, (b) convex, and (c) concave.

2.7. Effect of lateral width of epicardial fat

In previous simulations, we had considered only variation in the depth of epicardial fat (F), which meant it was considered to have limitless lateral width. In the present study we considered that the epicardial fat layer had limited lateral width (δ), as shown in Figure 5. The idea was to check the robustness of the new procedure, i.e. the impedance measurement should remain close to the value obtained without variation in the fat lateral width when δ was changed. For this part of the study, only the uniform fat profile was considered. The simulations were performed by decreasing the lateral width (δ) at intervals of 2 mm from 18.5 to 0.5 mm, simultaneously increasing the value of F from 1 to 6 mm (at intervals of 1 mm).

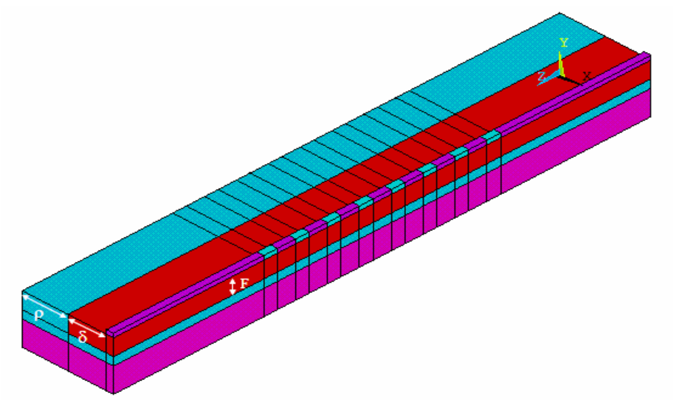

Figure 5. Model used to study the effect of lateral width of epicardial fat (δ) on the measured impedance. ρ: lateral width of atrial tissue; F: epicardial fat layer thickness.

3. Results

3.1. Construction of the model

The optimum outer dimensions were R = 20 mm, B = 6 mm, L = 118 mm and P = 33 mm. The convergence test provided a grid size of 0.3 mm in the finest zone (interface between fat and multi-electrode probe). We also checked the grid size away from the multi-electrode probe. The models had nearly 95,510 nodes and used over 524,000 tetrahedral elements.

3.2. Effect of different fat profiles

Figure 6 shows the impedance values for the different cases of fat profiles when the epicardial fat thickness varied between 1 and 6 mm. In the case of uniform fat profile (see Figure 6(a)), we observed that increasing F from 1 to 6 mm involved an increase in the impedance value, which was almost identical for all impedance measurements: Z_A increased from 103.6 Ω to 1223.3 Ω, Z_B from 103.5 Ω to 1218.4 Ω, Z_C from 103.4 Ω to 1218.6 Ω, etc.

Using the other fat profiles gave similar results: impedance readings decreased as maximum fat thickness was reduced. We also noticed that the impedance profiles followed a linear, convex and concave trend, respectively (Figure 6(b), 6(c) and 6(d)). Thus, for an F = 6 mm, with linear fat profile (Figure 6(b)), the impedance value decreased linearly from Z_A = 917.7 Ω to Z_E = 182.7 Ω. In the case of convex fat profile (Figure 6(c)) impedance decreased from Z_A = 542.9 Ω at the edge to Z_C = 135.6 Ω at the centre and then increased to Z_E = 610 Ω at the other edge. Finally, in the presence of a concave fat profile (Figure 6(d)), impedance increased from Z_A = 534.6 Ω to Z_C = 823.5 Ω and decreased to Z_E = 447 Ω. In conclusion, each impedance profile matched well with the corresponding fat profile.

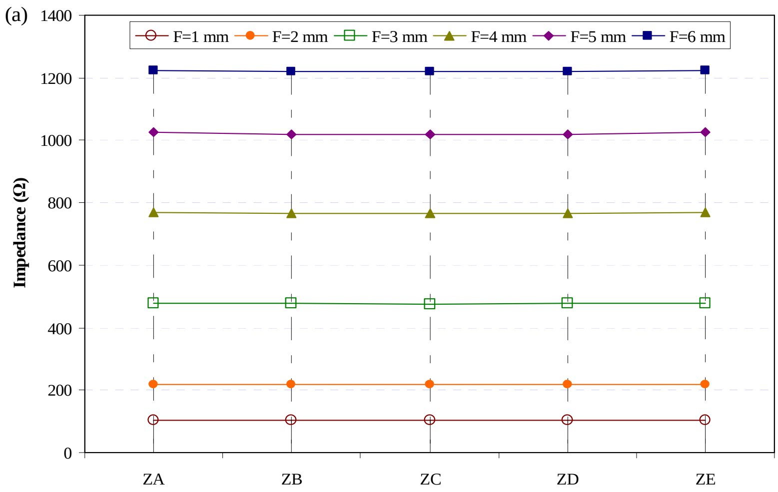

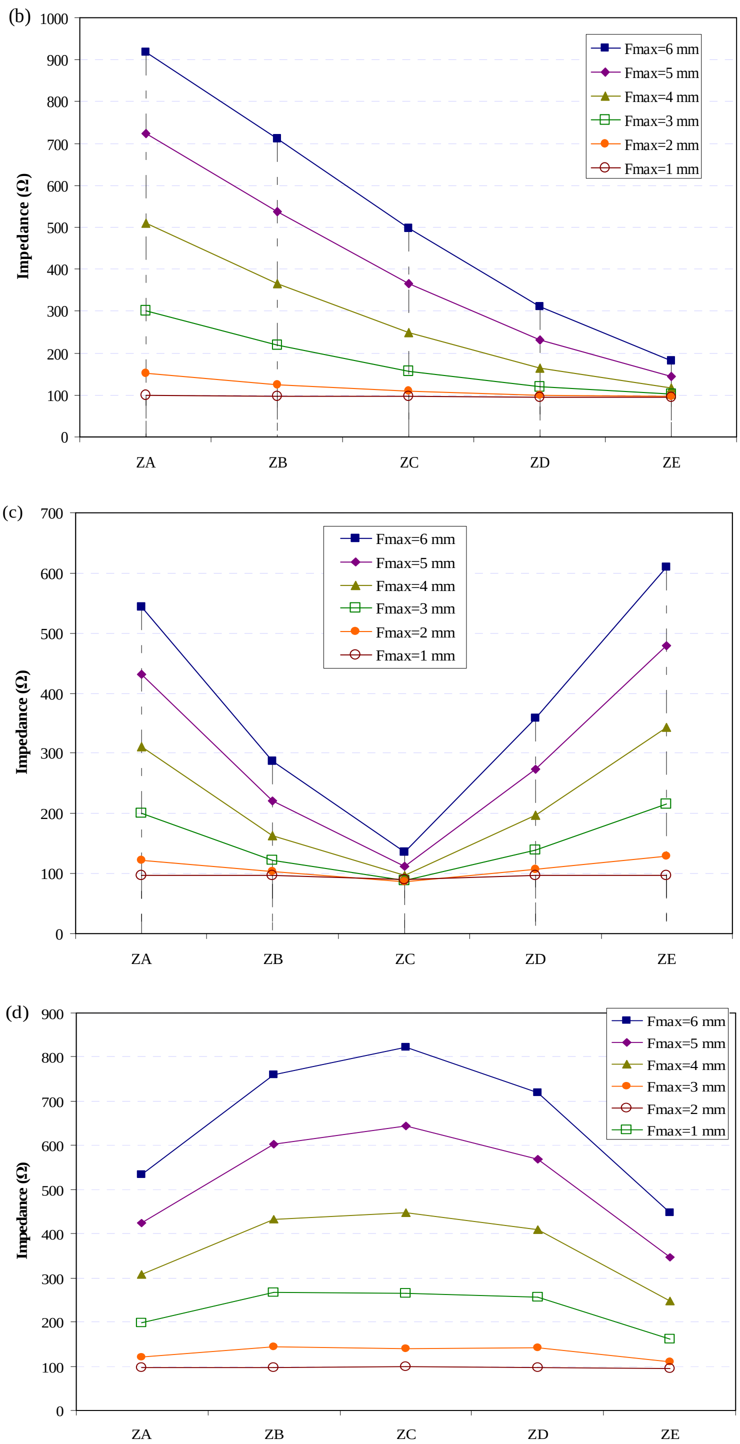

Figure 6. Impedance calculated for uniform (a), linear (b), convex (c), and concave (c) fat profiles.

3.3. Effect of lateral width of epicardial fat

Figure 7 shows the impedance values obtained by decreasing the lateral width of epicardial fat. We observed that decreasing fat lateral width (δ) involved a drop in the impedance reading, regardless of fat thickness. This effect was almost negligible for fat lateral widths > 4.5 mm, especially in the case of thin fat layers: the impedance value fell from 103.4 Ω to 101.4 Ω for the case of a 1 mm thin fat layer, while it dropped from 1218.6 Ω to 1010.5 Ω in the presence of a 6 mm thick fat layer. In contrast, this effect was more marked with smaller lateral widths (2.5 and 0.5 mm). For instance, with 6 mm of fat thickness impedance fell from 1218.6 Ω to 673.1 Ω for a lateral width of 2.5 mm and to 188.9 Ω for 0.5 mm.

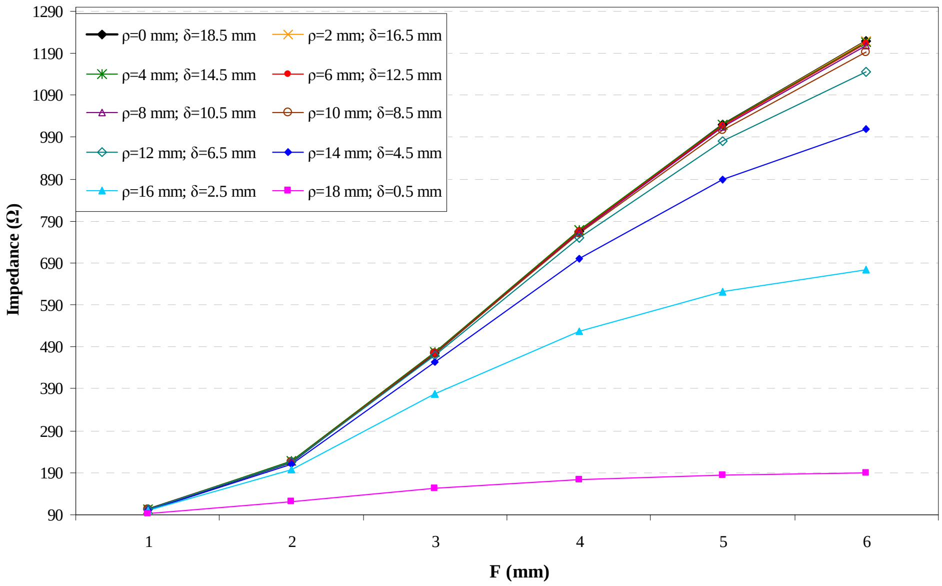

Figure 7. Impedance measurements by changing the lateral width of epicardial fat (δ) and the epicardial fat layer thickness (F).

4. Discussion

Previous RF ablation studies showed the difficulty of ablating the atrial wall underneath a thick epicardial fat layer (González-Suárez *et al* 2009). We therefore proposed to conduct a feasibility study on a new technique based on impedance measurements to asses the thickness of the epicardial fat prior to RF cardiac ablation. This could improve the ablative technique in general, since a particular RF power delivery protocol could be chosen, or even a particular kind of HIFU, microwave or cryoablation energy in order to optimize the thermal lesion according to the amount of epicardial fat present.

In this study we showed that impedance readings varied with the quantity of fat present under the electrodes. This increase in impedance with epicardial fat thickness was obviously due to the lower electrical conductivity of the epicardial fat (0.025 S/m) as compared to atrial tissue (0.4 S/m). These results are in agreement with the computer-simulation results obtained by Berjano and Hornero (2004) using a two-dimensional mathematical model.

We also observed that the fat profile under the electrodes followed the same trend as the impedance measurement (see Figure 6). Our results showed that Z_A for concave fat profile was similar to Z_A for the case of convex fat profile ($\approx$ 550 Ω). This was due to the fact that the impedance map covers only the tissue zone between electrodes 2 and 7, which means that the fat quantity under electrodes 2 and 3, i.e. those determining the Z_A value, is similar for the two fat profiles (see Figure 3).

Although the measurements were initially conducted by considering a fat layer with limitless lateral width, we conducted additional simulations to check whether the results would change in a real situation with limited fat width. Here again, our results showed that impedance values remained close to the results obtained previously for fat lateral widths over 4.5 mm (see Figure 7). This suggests that the proposed technique could fail when the multi-electrode probe is placed on epicardial fat with a thin lateral width (less than 4.5 mm).

The model proposed in this study is the first step in assessing epicardial fat prior to RF ablation and has certain limitations. On one hand, we only considered a multi-electrode probe with a rectangular section. Although this type of geometry could present a marked edge effect (Grimmes and Martinsen 2008), it was chosen because the ANSYS modeling technique was easier to implement. Future work should consider a probe with a more realistic geometry, such as a circular section and other factors such as electrode/tissue pressure could be included in the model, especially in the case of circular section probes. From a modeling point of view, this could be done by increasing the electrode insertion depth in the tissue.

Conclusions

The computational results suggest that measuring impedance could be a practical method of assessing epicardial fat prior to intraoperative cardiac ablation, i.e. “to map” the amount of adipose tissue under the probe. This is based on the fact that the impedance profiles obtained approximately coincided with the profiles of epicardial fat present under the electrodes of the probe.

Acknowledgments

This work was supported by a research grant from the Spanish Government in the “Plan Nacional de I+D+I del Ministerio de Ciencia e Innovación” (TEC2008-01369/TEC). The English revision and correction of this paper was funded by the Universidad Politécnica de Valencia, Spain.

References

Ba M, Fornés P, Nutu O, Latrémouille C, Carpentier A and Chachques J C 2008 Treatment of atrial fibrillation by surgical epicardial ablation: bipolar radiofrequency versus cryoablation *Arch. Cardiovasc. Dis.* **101** 763-8

Benjamin E J, Levy D, Vaziri S M, D'Agostino R B, Belanger A J and Wolf P A 1994 Independent risk factors for atrial fibrillation in a population-based cohort. The Framingham Heart Study *JAMA* **271** 840-4

Berjano E J and Hornero F 2004 Thermal-electrical modeling for epicardial atrial radiofrequency ablation *IEEE Trans. Biomed. Eng*. **51** 1348-57

Berjano E J and Hornero F 2005 A cooled intraesophageal balloon to prevent thermal injury during endocardial surgical radiofrequency ablation of the left atrium: a finite element study *Phys. Med. Biol.* **50** 269-79

Berjano E J and Hornero F 2006 Esophageal temperature during radiofrequency catheter ablation of left atrium: a three-dimensional computer modeling study *J. Cardiovasc. Electrophysiol.* **17** 405-10

Brankov J G, Danchev D M and Tonchev N S 2000 Theory of critical phenomena in finite-size systems. Scarling and quantum effects (Singapore: World Scientific)

Cox J L, Schuessler R B, Lappas D G and Boineau J P 1996 An 8 1/2-year clinical experience with surgery for atrial fibrillation *Ann. Surg*. **224** 267-73

Deneke T, Khargi K, Müller K M, Lemke B, Mügue A, Laczkovics A, Becker A E and Grewe P H 2005 Histopathology of intraoperatively induced linear radiofrequency ablation lesions in patients with chronic atrial fibrillation *Eur. Heart J.* **26** 1797-803

Doss J D 1982 Calculation of electric fields in conductive media *Med. Phys.* **9** 566-73

Dumas J H, Himel H D, Kiser A C, Quint S R and Knisley S B 2008 Myocardial electrical impedance as a predictor of the quality of RF-induced linear lesions *Physiol. Meas.* **29** 1195-207

Gabriel S, Lau R W and Gabriel C 1996 The dielectric properties of biological tissues: III. Parametric models for the dielectric spectrum of tissues *Phys. Med. Biol.* **41** 2271-93

Geddes L A 1989 Detection of physiological events by impedance. Principles of Applied Biomedical Instrumentation *Wiley Interscience* **1** 276-410

González-Suárez A, Berjano E J and Hornero F 2009 Assessment of the epicardial fat prior to RF cardiac ablation: concept proof using computational modeling *Proc. of the XXVII Ann. Meeting of the Biomedical Engineering Spanish Society* (*Cádiz, Spain)* pp 279-82.

González-Suárez A, Hornero F and Berjano E J 2010 Mathematical Modeling of Epicardial RF Ablation of Atrial Tissue with Overlying Epicardial Fat *TOBEJ* **4** 47-55

Grimmes S and Martinsen O G 2008 *Bioimpedance and Bioelectricity Basics* 2nd edn (Oxford: Academic Press)

Hong K N, Russo M J, Liberman E A, Trzebucki A, Oz M C, Argenziano M and Williams M R 2007 Effect of epicardial fat on ablation performance: a three-energy source comparison *J. Card. Surg*. **22** 521-4

Kannel W B, Wolf P A, Benjamin E J and Levy D 1998 Prevalence, incidence, prognosis, and predisposing conditions for atrial fibrillation: population-based estimates *Am. J. Cardiol*. **82** 2N-9N

Khargi K, Hutten B A, Lemke B and Deneke T 2005 Surgical treatment of atrial fibrillation; a systematic review *Eur. J. Cardiothorac. Surg*. **27** 258-65

Mitnovetski S, Almeida A A, Goldstein J, Pick A W and Smith J A 2009 Epicardial high-intensity focused ultrasound cardiac ablation for surgical treatment of atrial fibrillation *Heart Lung Circ.* **18** 28-31

Miyagi Y, Ishii Y, Nitta T, Ochi M and Shimizu K 2009 Electrophysiological and histological assessment of transmurality after epicardial ablation using unipolar radiofrequency energy *J. Card. Surg*. **24** 34-40

Nakajima H, Kobayashi J, Bando K, Niwaya K, Tagusari O, Sasako Y, Nakatani T and Kitamura S 2002 The effect of cryo-maze procedure on early and intermediate term outcome in mitral valve disease: case matched study *Circulation* **106** I46-50

Pruitt J C, Lazzara R R. and Ebra G 2007 Minimally invasive surgical ablation of atrial fibrillation: The thoracoscopic box lesion approach *J. Interv. Card. Electrophysiol.* **20** 83-7

Santiago T, Melo J Q, Gouveia R H and Martins A P 2003a Intra-atrial temperatures in radiofrequency endocardial ablation: histologic evaluation of lesions *Ann. Thorac. Surg.* **75** 1495-501

Santiago T, Melo J, Gouveia R H, Abecasis L M, Adragão P and Martins A P 2003b Epicardial radiofrequency applications: in vitro and in vivo studies on human atrial myocardium *Eur. J. Cardiothorac. Surg*. **24** 481-6

Wolf P A, Abbott R D and Kannel W B 1991 Atrial fibrillation as an independent risk factor for stroke: the Framingham Study *Stroke* **22** 983-8